Contrib Mineral Petrol (2011) 162:651–669
DOI 10.1007/s00410-010-0596-x

ORIGINAL PAPER

Magma mixing in the 1100 AD Montaña Reventada composite lava flow, Tenerife, Canary Islands: interaction between rift zone and central volcano plumbing systems

S. Wiesmaier · F. M. Deegan · V. R. Troll · J. C. Carracedo · J. P. Chadwick · D. M. Chew

Received: 8 April 2010 / Accepted: 15 November 2010 / Published online: 3 February 2011

Abstract Zoned eruption deposits commonly show a lower felsic and an upper mafic member, thought to reflect eruption from large, stratified magma chambers. In contrast, the Montaña Reventada composite flow (Tenerife) consists of a lower basanite and a much thicker upper phonolite. A sharp interface separates basanite and phonolite, and chilled margins at this contact indicate the basanite was still hot upon emplacement of the phonolite, i.e. the two magmas erupted in quick succession. Four types of mafic to intermediate inclusions are found in the phonolite. Inclusion textures comprise foamy quenched ones, others with chilled margins and yet others that are physically mingled, reflecting progressive mixing with a decreasing temperature contrast between the end-members. Analysis of basanite, phonolite and inclusions for majors, traces and Sr, Nd and Pb isotopes show the inclusions to be derived from binary mixing of basanite and phonolite end-members in ratios of 2:1 to 4:1. Although, basanite and phonolite magmas were in direct contact, contrasting $^{206}Pb/^{204}Pb$ ratios show that they are genetically distinct (19.7193(21)–19.7418(31) vs. 19.7671(18)–19.7807(23), respectively). We argue that the Montaña Reventada basanite and phonolite first met just prior to eruption and had limited interaction time only. Montaña Reventada erupted from the transition zone between two plumbing systems, the phonolitic Teide-Pico Viejo complex and the basanitic Northwest rift zone. A rift zone basanite dyke most likely intersected the previously emplaced phonolite magma chamber. This led to eruption of geochemically and texturally unaffected basanite, with the inclusion-rich phonolite subsequently following into the established conduit.

Keywords Magma mixing · Basanite · Phonolite · Tenerife · Canary Islands · Reventada

Communicated by J. Hoefs.

Electronic supplementary material The online version of this article (doi:10.1007/s00410-010-0596-x) contains supplementary material, which is available to authorized users.

S. Wiesmaier (✉) · D. M. Chew
Department of Geology, Trinity College Dublin,
2 College Green, Dublin 2, Ireland
e-mail: wiesmais@tcd.ie

F. M. Deegan · V. R. Troll
Department of Earth Sciences, Uppsala University,
Villavägen 16, 75236 Uppsala, Sweden

J. C. Carracedo
Estación Volcanológica de Canarias, IPNA-CSIC,
Av. Astrofísica Francisco Sanchez 3,
38206 La Laguna, Tenerife, Spain

J. P. Chadwick
Department of Petrology (FALW), Vrjie Universiteit,
1081 HV Amsterdam, The Netherlands

Introduction

The key issues for understanding magma mixing in a given deposit are whether or not the distinct magmas co-existed for any appreciable amount of time in a stratified magma chamber prior to eruption and whether they are co-genetic. Co-genetic, stratified magma chambers have frequently been hypothesised in the context of large ignimbrite eruptions (e.g. Sparks et al. 1977; Blake 1981a; Huppert et al. 1982; Wolff and Storey 1984; Blake and Ivey 1986; Freundt and Schmincke 1992; Calanchi et al. 1993; Araña et al. 1994; Kuritani 2001; Troll and Schmincke 2002).

However, co-genetic magmas, which develop vertical chemical gradients with time, seem to be restricted to relatively large magma chambers (Smith and Bailey 1966; Smith 1979; Hildreth 1979, 1981). Alternatively, the origin of mixed magmas has also been explained by the forced intrusion or fountaining of a genetically distinct magma into another, whereby the newly arriving magma may trigger an eruption due to super-heating and re-mobilisation (e.g. Turner 1980; Campbell and Turner 1986; Turner and Campbell 1986; Eichelberger et al. 2000; Izbekov et al. 2004; Troll et al. 2004). For example, Izbekov et al. (2004) suggested that a mafic dyke had dissected a resident andesite magma chamber, triggering the intermittent eruption of a range of mixed products at Karymsky volcano, Kamchatka in 1996.

Here, we focus on the Montaña Reventada lava flow (895 ± 155 year BP; Carracedo et al. 2007), one of the most recent deposits within the post-Icod-La Guancha-collapse succession in Tenerife. A basanite lava erupted just prior to a phonolite lava, the latter of which contains abundant dark inclusions, to form a composite flow or cooling unit. Earlier studies on Montaña Reventada (Araña et al. 1989, 1994) provided mass balance calculations that, combined with mineral abundances, allowed them to exclude continuous closed system fractional crystallisation as an origin for these inclusions, supporting a hybrid (mixing) origin instead. Due to a lack of mingling textures within the phonolite matrix, they explained the origin of intermediate inclusions exclusively through diffusional hybridisation. In consequence, the model of Araña et al. (1994) required a diffusional interface between basanite and phonolite in the magma chamber, which would span the entire compositional range between basanite and phonolite. This interface would have to have persisted for an extended period of time to allow for the significant compositional variation of the inclusions (cf. Crank 1975; Baker 1990). Furthermore, to account for the fact that the basanite erupted first (although it should have ponded underneath the phonolite in the magma chamber), their model employed a reduction in basanite density below that of the phonolite. In their view, this would be achieved by thermal equilibration between basanite and phonolite and resultant crystallisation within the basanite, therefore suggesting a relatively long-lived and stably stratified magma chamber (cf. Araña et al. 1994).

Here, we merge our new geochemical data with that of Araña et al. (1994) and provide new isotope data. By presenting a reliable, geochemically coherent dataset along with a detailed textural analysis of inclusion types, we are able to provide a refined mixing model that is consistent with field and textural constraints. This allows for a substantial revision of the magmatic processes at work and the consequent dynamics envisaged for the Montaña Reventada eruption, implying the interaction of distinct magma plumbing systems in Tenerife.

The Montaña Reventada lava flow

In Tenerife, Canary Islands, the Teide-Pico Viejo stratovolcano complex is located at the junction between two active rift zones, one to the Northwest, the other to the Northeast (Carracedo 1994; Carracedo et al. 2007). Montaña Reventada consists of a group of vents located within the Northwest rift zone (Carracedo et al. 2007). Two exceptional roadcut sections at 330437/3128642 (UTM 28R ± 15 m) at either side of the road TF-38 (locally referred to as “Carretera Boca Tauce—Chío”) provide a cross-section through the complete stratigraphy of this eruption, including the bottom contact with older lavas (Fig. 1). This roadcut, downhill from the Las Cañadas Caldera, has been previously described by Araña et al. (1994). After passing Montaña Samara, the road leads into a wide left turn through the Montaña Reventada lava flow. From bottom to top, the Montaña Reventada stratigraphy comprises the following components: (i) A red bottom breccia of about 10–20 cm thickness, composed of scoriaceous basanite, which is scarcely porphyritic and shows flow banding in parts. (ii) A lower basanite layer of variable thickness (20–200 cm), composed of massive, dark, mainly aphyric lava showing flow banding that is occasionally folded over. Vertical cooling cracks are abundant (Fig. 1a). In places, the massive parts grade into welded scoria, where the scoria clasts are of variable vesicularity. At 1–2 km downhill from the outcrop described here, the basanite contains abundant plagioclase. (iii) An upper phonolite layer of 10–12 m thickness that is massive, light coloured and porphyritic. The contact between the basanite and the overlying phonolite is smooth and undulating, lacking top or basal brecciation. In places, the phonolite intrudes the lower basanite or appears to “lift out” basanite blocks (up to 50 cm). In one case, a cooling fracture of the underlying basanite appears to have been filled with phonolite (Fig. 1d). Here, the basanite shows a chilled margin against the intruding phonolite. Cooling joints in the phonolite are less pronounced than in the basanite. In the first metre above the basanite–phonolite contact, vesicles up to 10 cm are abundant. These are elongate and parallel to the contact and grade into equant shapes at about 40 cm above the contact. The phonolite hosts frequent dark inclusions that range in size from a few cm to 50 cm across and appear to gradually decrease in abundance up-section. The phonolite becomes pink in the uppermost half metre (oxidised top). (iv) A top breccia to the phonolite of up to 1.5 m in thickness consists of large clinker and glassy blocks.

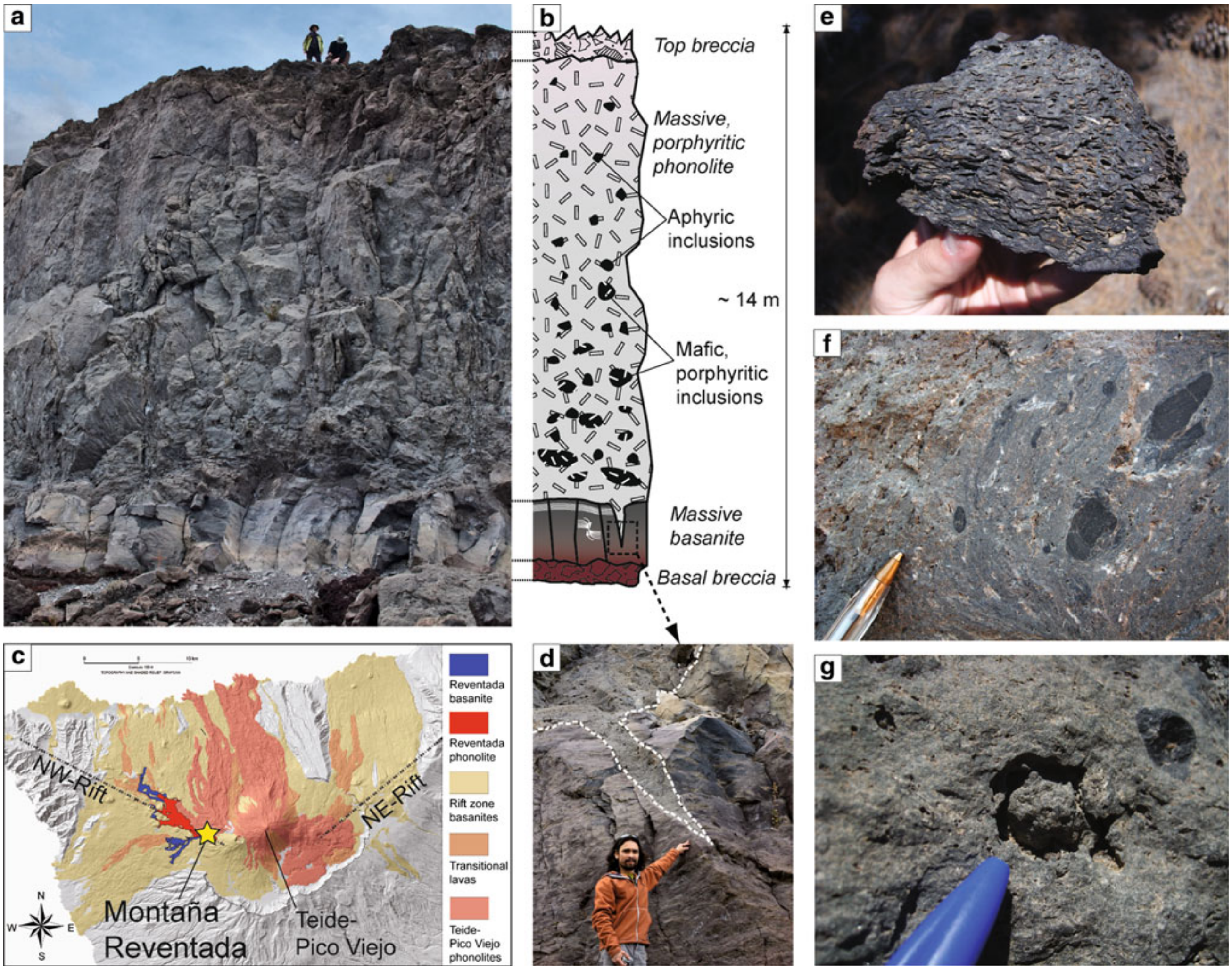

Fig. 1 **a** A photograph of the main outcrop of the Montaña Reventada composite flow with people for scale, **b** a simplified stratigraphic column of this main outcrop, **c** a location map after Carracedo et al. (2007) and **d** opened fracture within the basanite that has been filled with phonolite. **e** Vesicle-rich and plagioclase-bearing basanite can be found at the flow front. **f** Mingled appearance of light-coloured inclusion. **g** Degassing halo around inclusion in host phonolite

Methodology

To define the lithological units and constrain the processes that gave rise to the Montaña Reventada composite eruption, 20 samples were analysed for their major and trace element concentrations as well as for their Sr, Nd and Pb isotopes. The compositional data are complemented by field and petrographical evidence from outcrop, hand-specimen and thin-sections.

Samples and sample selection

The sample set is stratigraphically constrained and comprises 14 whole-rock and six groundmass samples. Three basanites, seven phonolites and four inclusions were selected for whole-rock analyses. Groundmass measurements encompassed two basanites and four phonolites. All samples are from the two road sections at TF-38.

Unweathered pieces of rock were cut and selected for whole-rock and groundmass analysis. The samples are young (895 ± 155 year BP, Carracedo et al. 2007) and overall very fresh. Nevertheless, cracks and rims affected by weathering were avoided. Samples were crushed in a jaw crusher and washed and hand-picked at Trinity College Dublin. Approximately 30 g of fresh, pristine chips were pulverised in a WC-TEMA mill.

Major and trace element analyses

The major element dataset was produced by XRF at IFM-GEOMAR, Kiel, Germany. Samples were dried at 110°C and analysed on fused beads using an automated Philips

PW1480 X-ray spectrometer. Lithium tetraborate glass fusion beads were prepared following the methods of Norrish and Hutton (1969), with modifications after Harvey et al. (1973) and Brian et al. (1980). All analyses were performed with an Rh tube, and calibration was performed using international geological reference samples (cf. Abratis et al. 2002). H_2O and CO_2 were determined by infra-red photometry (Rosemount CSA 5003) after heating the rock powder to 960°C.

Trace element analyses by ICP-MS were carried out at the Department of Petrology (FALW), Vrjie Universiteit, Amsterdam, Netherlands. Samples were prepared using a modified version of the method described by Turner et al. (1999).

Samples and geological standards were prepared as 1:5,000 measuring solutions in 5% HNO_3 for running on a Quadrupole Thermo X-Series II ICPMS following the method given in Eggins et al. (1997). Detection limits and analytical precision range from < 100 ppb to < 1 ppt, and relative analytical precision is typically between ~ 5 and 10% (one standard deviation). Results are listed in Table 1 and in the online resource (Table A1).

Radiogenic isotope analyses

Isotopes of Sr, Nd, and Pb were determined at the Vrije Universiteit, Amsterdam following standard chemical separation techniques (Pin et al. 1994; Elburg et al. 2005). Sr samples of 500 ng each were loaded onto single annealed Re filaments with $TaCl_5$. Sr isotope ratios were measured using a Finnigan MAT 262 system operating in static mode. The data were corrected for instrumental mass fractionation using an exponential law normalised to $^{86}Sr/^{88}Sr = 0.1194$. Long-term replicate analyses of NBS 987 gave a mean $^{87}Sr/^{86}Sr$ ratio of 0.710230(9) ($n = 77$). The BHVO-2 standard gave a $^{87}Sr/^{86}Sr$ ratio of 0.703417(9), compared to 0.703435 reported by Raczek et al. (2003). The maximum estimated blank contribution is significantly less than 0.1%, and thus no blank corrections have been made to the data.

Nd and Pb samples were prepared as 400–800 ppb measuring solutions in 4 ml 1% HNO_3 for measurement on a Finnigan Neptune Multi-Collector ICP-MS (MC-ICPMS). The method used to measure Nd isotope ratios is given in Luais et al. (1997). During the course of analyses, the CIGO internal standard gave a mean $^{143}Nd/^{144}Nd$ ratio of 0.51134(4) ($n = 10$). The BHVO-2 standard gave a ratio of 0.51298(5), which agrees well with the ratio reported by Raczek et al. (2003). Pb isotopes were analysed using the standard-sample bracketing method given in Elburg et al. (2005). The NBS 981 standard gave mean $^{206}Pb/^{204}Pb$, $^{207}Pb/^{204}Pb$ and $^{208}Pb/^{204}Pb$ ratios of 16.9435(14), 15.5017(20) and 36.7297(30), respectively ($n = 2$). Two BHVO-2 measurements gave mean $^{206}Pb/^{204}Pb$, $^{207}Pb/^{204}Pb$ and $^{208}Pb/^{204}Pb$ ratios of 18.6252(16), 15.5392(20) and 38.2269(34), respectively, compared to 18.6474(242), 15.5334(94) and 38.2367(182) reported, respectively, by Weis et al. (2006). All errors are reported as 2SD.

Results

Petrography

Basanite

Plagioclase phenocrysts and vesicles are abundant in the distal parts (the flow front) of the basanite lava flow. In contrast, at the main outcrop described here, Reventada basanite is essentially aphyric and vesicle free. However, scarce plagioclase phenocrysts are occasionally present (Table 2). The microcrystalline, melanocratic groundmass consists of lath-shaped plagioclase, mafic pyroxene microlites with high birefringence colours and opaque Fe/Ti oxides. The groundmass shows abundant flow lamination, which in places is extensively folded over (Fig. 2a).

Phonolite

The overlying phonolite is porphyritic, containing 10% feldspar phenocrysts, 3% opaque minerals, along with rare clinopyroxene and amphibole. The amphibole crystals display opaque dehydration rims. Feldspar may be intergrown with opaque minerals and, less frequently, with pyroxene and opaque minerals. Feldspars are of alkaline composition (Table 2) and usually single, euhedral crystals with rounded corners and abundant Carlsbad twinning or, less often, glomerocrysts (<10 mm). Larger crystals tend to display sieve textures.

Microcrystalline, leucocratic phonolite groundmass is holocrystalline and consists mainly of feldspar and opaque minerals. Vesicles are abundant and make up ~ 10 vol% of the rock close to the contact with the lower basanite, but decrease to ~ 1 vol% farther away from the basanite (Fig. 2c).

Inclusions

Inclusion textures range from frothy and vesicle rich to scarcely porphyritic and banded to porphyritic and mingled. Four major types are distinguished. Type I: scarcely feldspar bearing and finely vesicular with a cryptocrystalline groundmass (dyktytaxitic texture, cf. Bacon 1986). They sometimes contain alkali feldspars with anhedral, relic appearance. This type of inclusion has angular outlines and is occasionally intruded by phonolite and, thus,

Table 1 Major and trace element and Pb isotope data for Montaña Reventada

(wt%)	Basanite					Inclusions				Phonolite
	205-1	205-2	205-3	205-1 gm	205-2 gm	E 206A	E 206B	E 206D	E 204F	206 Cont
SiO_2	46.63	46.2	46.19	46.86	46.71	50.08	50.12	50.44	48.4	57.46
TiO_2	3.31	3.35	3.33	3.32	3.36	2.62	2.64	2.6	2.92	1.35
Al_2O_3	17.16	17.13	17.14	17.18	17.17	17.65	17.68	17.74	17.65	18.49
Fe_2O_3	11.13	11.22	11.21	11.09	11.19	9.04	9.04	9.02	9.84	5.3
MnO	0.18	0.18	0.18	0.18	0.18	0.18	0.18	0.18	0.21	0.17
MgO	4.42	4.53	4.55	4.48	4.58	3.35	3.44	3.39	3.75	1.46
CaO	9	9.15	9.12	9.06	9.14	6.91	7.01	6.89	7.72	2.89
Na_2O	4.94	4.97	4.93	4.83	4.86	6.3	6.05	6.07	5.67	7.59
K_2-O	1.92	1.85	1.88	1.91	1.91	2.46	2.62	2.66	1.75	4.32
P_2O_5	1.26	1.29	1.3	1.29	1.29	0.99	1	1	1.17	0.4
H_2O	0.08	0.09	0.09			0.12	0.14	0.08	0.24	0.17
CO_2	0.02	0.02	0.02			0.02	0.02	0.01	0	0.04
Sum	100.28	100.17	100.13	100.51	100.7	99.91	100.1	100.29	99.45	99.69
(ppm)										
Ba	581.9	728.4	528.8	526.1	616.2	780.3	594.6	708.7	1,053.7	668.5
Sr	982.1	1,327.3	936.7	910.3	1,068.2	968.5	767.4	885.2	1,075.5	239.6
Hf	7.04	8.53	5.95	6.29	7.32	8.28	6.65	8.43	6.53	7.68
Th	6.48	8.59	6.32	5.59	7.21	11.07	7.68	11.09	6.36	8.97
U	1.90	2.19	1.55	1.68	1.86	2.43	2.00	2.49	1.59	2.79
Nb	82.3	115.3	77.5	81.3	99.8	113.4	93.3	110.3	110.8	113.8
Ta	5.75	7.20	4.63	4.87	5.54	7.07	5.64	6.74	6.05	6.41
Rb	39.50	36.31	29.89	36.00	33.18	58.16	47.98	53.57	25.93	64.70
Pb	3.52	4.09	2.88	3.18	3.62	5.43	4.12	5.32	3.53	5.53
$^{206}Pb/^{204}Pb$	19.7418 (16)	19.7401 (10)	19.7355 (7)	19.7377 (9)	19.7193 (10)	19.7641 (12)	19.7528 (7)	19.7594 (7)	19.7660 (8)	19.7671 (9)
$^{207}Pb/^{204}Pb$	15.6122 ‘(17)	15.6163 (9)	15.6213 (9)	15.6173 (16)	15.6146 (17)	15.6196 (15)	15.6117 (8)	15.6175 (8)	15.6142 (9)	15.6168 (15)
$^{208}Pb/^{204}Pb$	39.5607 (31)	39.5673 (20)	39.5720 (14)	39.5638 (18)	39.5423 (22)	39.5858 (23)	39.5603 (15)	39.5786 (14)	39.5701 (16)	39.5769 (19)

(wt%)	Phonolite									
	206-2	206-3	206-5	206-2 gm	206-5 gm	207-4	207-5	207-6	207-4 gm	207-6 gm
SiO_2	58.68	59.12	57.65	59.31	57.82	58.88	58.17	58.75	59.16	58.86
TiO_2	1.08	1.03	1.28	1.06	1.28	1.1	1.21	1.12	1.08	1.11
Al_2O_3	18.53	18.61	18.58	18.63	18.52	18.58	18.5	18.51	18.55	18.47
Fe_2O_3	4.56	4.41	5.09	4.54	5.09	4.54	4.99	4.57	4.53	4.76
MnO	0.16	0.16	0.17	0.16	0.17	0.17	0.16	0.16	0.17	0.17

Table 1 continued

(wt%)	Phonolite									
	206-2	206-3	206-5	206-2 gm	206-5 gm	207-4	207-5	207-6	207-4 gm	207-6 gm
MgO	1.05	1	1.33	1.04	1.35	1.09	1.28	1.12	1.06	1.12
CaO	1.99	1.87	2.65	1.97	2.63	1.98	2.35	2.1	1.96	2.08
Na_2O	7.91	7.85	7.7	7.9	7.64	7.67	7.67	7.81	7.73	7.88
K_2-O	4.75	4.81	4.42	4.82	4.52	4.73	4.57	4.66	4.83	4.74
P_2O_5	0.29	0.28	0.37	0.29	0.38	0.29	0.35	0.31	0.29	0.32
H_2O	0.09	0.1	0.09			0.16	0.26	0.2		
CO_2	0	0	0.01			0.02	0.01	0.02		
Sum	99.24	99.4	99.5	99.98	99.67	99.29	99.52	99.37	99.6	99.76
(ppm)										
Ba	996.9	1,289.7	881.1	789.1	796.4	975.8	1,055.4	1,032.9	839.8	694.3
Sr	186.7	218.4	274.0	154.2	270.4	171.3	244.7	203.0	159.1	155.6
Hf	10.86	13.18	9.35	10.79	10.71	9.59	10.07	9.31	11.10	7.83
Th	14.90	19.87	12.27	12.45	12.57	13.99	15.06	11.83	14.87	10.63
U	3.71	4.68	3.28	3.29	3.49	3.58	3.73	2.75	3.75	2.33
Pb	8.52	10.04	6.28	7.28	6.59	7.10	7.44	6.04	7.65	4.64
Ta	8.75	10.39	7.51	8.14	8.20	8.28	8.17	7.85	8.43	6.01
Rb	101.62	116.55	79.90	91.25	95.38	90.05	97.71	86.14	91.28	62.88
Pb	8.91	10.93	7.34	8.18	7.93	8.27	8.57	6.75	8.67	5.25
$^{206}Pb/^{204}Pb$	19.7807 (11)	19.7762 (6)	19.7746 (6)	19.7723 (6)	19.7708 (10)	19.7767 (8)	19.7761 (7)	19.7802 (7)	19.7723 (10)	19.7750 (12)
$^{207}Pb/^{204}Pb$	15.6232 (14)	15.6175 (9)	15.6189 (8)	15.6178 (8)	15.6195 (15)	15.6219 (10)	15.6210 (9)	15.6210 (9)	15.6203 (16)	15.6209 (17)
$^{208}Pb/^{204}Pb$	39.5997 (23)	39.5845 (14)	39.5882 (13)	39.5835 (14)	39.5843 (22)	39.5980 (18)	39.5929 (14)	39.5983 (15)	39.5873 (22)	39.5931 (25)

Please note that additional trace element data along with Sr and Nd isotope data can be found in the online resource (Table A1). Samples with number 205 are from the basanite. 206Cont is the phonolite sample just above the contact between basanite and phonolite. Samples with number 207 are from the top of the phonolite layer, 206 samples are from the bottom of the phonolite. "gm" in a sample name denotes a groundmass sample

Table 2 Feldspar microanalyses of Montaña Reventada samples (Wiesmaier 2010)

Sample	Basanite REV-71	Inclusion REV-63		Phonolite REV-85b
	Plagioclase	Plagioclase	Alkali feldspar	Alkali feldspar
(mol%)				
An	38.85	32.85	5.41	5.95
Ab	57.17	63.27	70.74	70.28
Or	3.98	3.88	23.85	23.77
(ppm)				
Rb	1.3	1.6	21.1	19.0
Ba	614.3	1,123.4	1,073.0	800.8
La	13.0	14.0	6.6	7.0
Ce	16.0	16.6	5.2	6.4
Pr	1.0	1.0	0.3	0.3
Nd	2.8	2.4	0.5	0.6
Eu	1.2	1.4	2.0	1.8
Y	0.3	0.4	0.2	0.3
Pb	1.8	2.5	4.3	4.1
Sr	2,522.9	2,330.8	37.4	31.5
Ti	636.0	550.0	588.2	554.3
Mg	191.1	153.3	–	–

Please note that a different sample set has been used for the analyses of feldspar phenocrysts. Major element analyses performed by electron microprobe. Trace element analyses carried out by LA-ICP-MS. Inclusions may contain both plagioclase and anorthoclase

appears to have behaved competently against the liquid phonolite groundmass (Fig. 2d, e), Type II: dark-coloured, feldspar-bearing inclusions with a lobate margin that sometimes features a chilled margin. Type II inclusions contain nodules of darker material (Fig. 2 f, g), Type III: lighter coloured than type II, feldspar-bearing inclusions that show a relatively coarser-grained groundmass of microlites of feldspars and amphiboles. These inclusions are blob-like, with lighter- and darker-coloured groundmass mingled with each other. Filaments and blobs of dark magma are visible in light-coloured type III inclusions. Glomerocrysts of feldspar intergrown with opaque oxides, clinopyroxene and amphibole infrequently occur. Inclusions of about 1 cm or less in size may show a sharp, well-defined contact or a diffuse transition between inclusion and phonolite material (Fig. 2 g, h), Type IV: dense inclusions with accessory feldspar that show flow banding. Phenocryst orientations generally appear to follow the observed groundmass lamination. Their contact to the host phonolite is sharp and angular (Fig. 2i).

Inclusions contain feldspar of anorthoclase composition and a range of plagioclase crystals with compositions ranging from labradorite to oligoclase. Their composition was determined by EMP as part of a parallel project (Wiesmaier 2010); a representative dataset is shown in Table 2. Photomicrographs of representative feldspar phenocrysts can be found in the online resource (Fig. A1).

Whole-rock and groundmass composition

Major elements

In the Total Alkali versus Silica diagram (TAS, LeBas et al. 1986), the lower lava layer is classified as a basanite and the upper as a phonolite, while inclusions contained within the phonolite occupy variable compositions between the two, plotting as either basanites, phonotephrites or tephriphonolites (Table 1, Fig. 3). Inclusion data from Araña et al. (1994) plot in the same linear, alkaline sequence between basanites and phonolites, albeit with somewhat higher alkali element concentrations.

Major element data from this study are broadly consistent with the data from Araña et al. (1994), when plotted in Harker diagrams (Fig. 4). All major elements form linear trends between basanite and phonolite. The gap between the two principal lava types is always bridged by inclusions of intermediate composition from both data sets.

Trace elements

In a multielement variation diagram normalised to primitive mantle, basanites and inclusions show very similar patterns; however, inclusions appear more enriched in the LILE Cs, Rb and Ba and the HFSE Th and U. Phonolites are more enriched than basanites in the LILE, but display a pronounced negative Sr and positive Zr anomaly and an

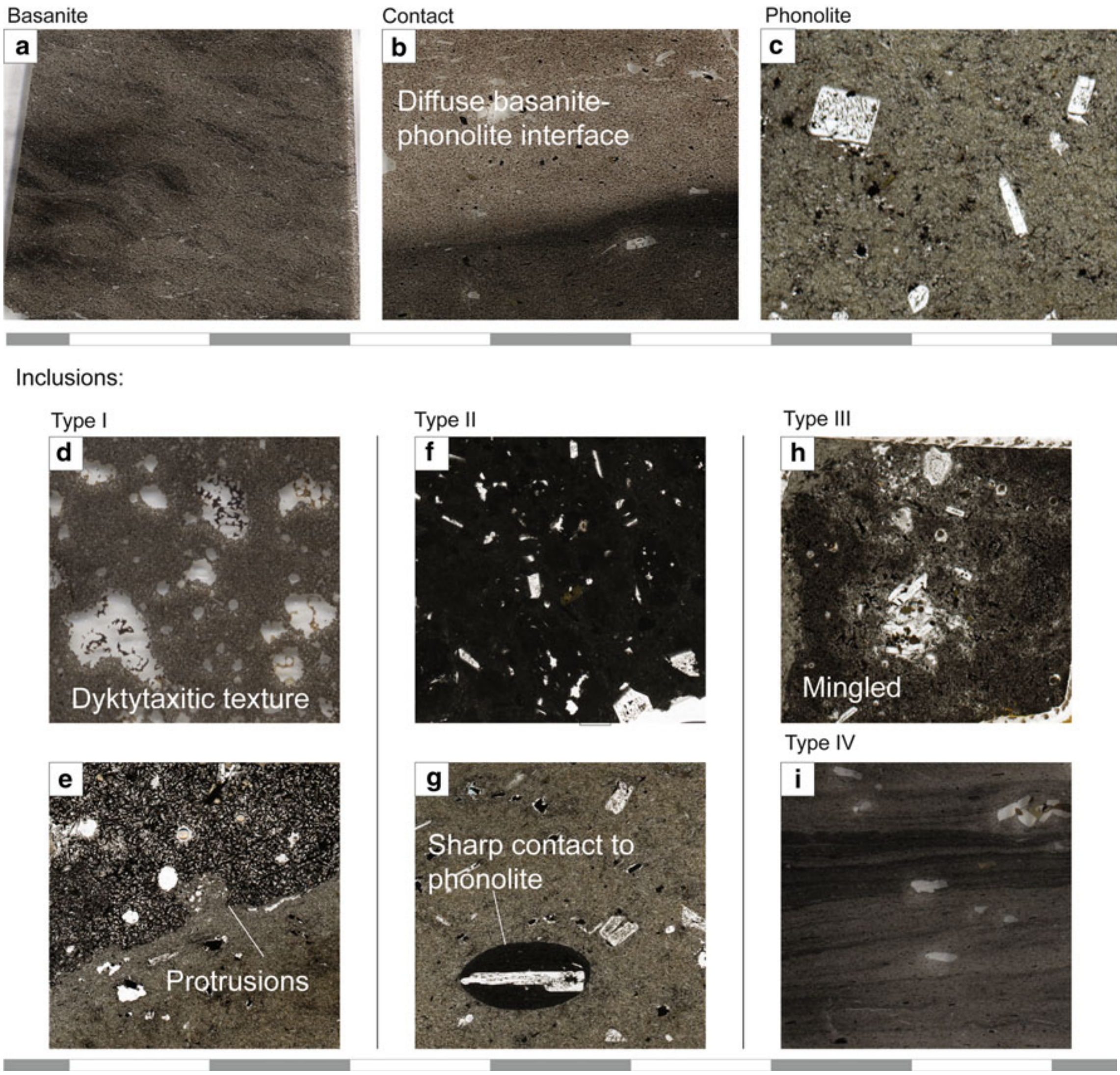

Fig. 2 Thin-section images of Montaña Reventada rocks (scans: **a**, **b**, **d**, **i**; photomicrographs: **c**, **e**, **f**, **g**, **h**). **a** Basanite, **b** diffuse contact between basanite and phonolite **c** phonolite, **d**, **e** type I inclusions, frothy and vesicle rich, **f**, **g** type II inclusions, crystal rich, chilled margin, **h** type III inclusions massive, crystal-rich, mingled, **i** type IV inclusions, flow-banded. *Scale bar* in 1-cm divisions. Sieve-textured feldspar occurs in all samples

overall depletion in MREE (Table 1, online resource Table A1 and Fig. A2).

When whole-rock trace element data are plotted against Zr concentration (cf. Wolff et al. 2000), basanites and phonolites again plot as end-members, with the inclusions generally filling the space between them. However, phonolites show a rather wide spread in several incompatible trace elements, while the basanites appear closer spaced (cf. Troll et al. 2004).

Isotope data

Basanite whole-rocks have $^{87}Sr/^{86}Sr$ values of between 0.0703032(9) and 0.703040(7) (groundmass: 0.0703024(10) to 0.703046(9)). The phonolite whole-rocks range from 0.703032(7) to 0.703062(9) (groundmass: 0.703032(9) to 0.703082(7)). The inclusions display values from 0.703032(7) to 0.703059(9).

Basanites show $^{143}Nd/^{144}Nd$ ratios from 0.512855(38) to 0.512896(46) and phonolites from 0.512848(42) to 0.512910(46). Inclusions show a range in Nd ratios between 0.512871(46) and 0.512899(42). All Nd ratios are within error of each other.

The $^{206}Pb/^{204}Pb$ ratios range from 19.7193(21) to 19.7418(31) versus 19.7528(14) to 19.7660(16) versus 19.7671(18) to 19.7807(23), for basanite, inclusions and phonolite, respectively, with significant differences among these three groups. In turn, basanite, inclusion and phonolite

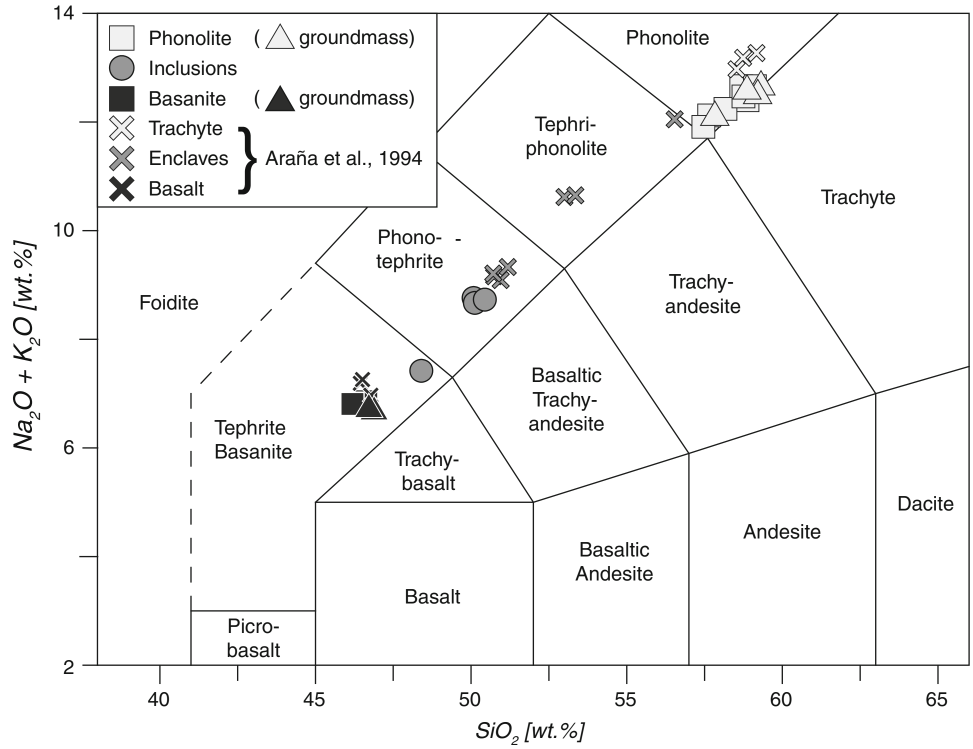

Fig. 3 Total alkali versus silica diagram after LeBas et al. (1986). The two principal lava types, basanite and phonolite, are end-members, while the inclusions are of variable intermediate compositions. The Araña et al. (1994) data (*crosses*) plot on the same linear trend as our samples, between the two principal lava compositions

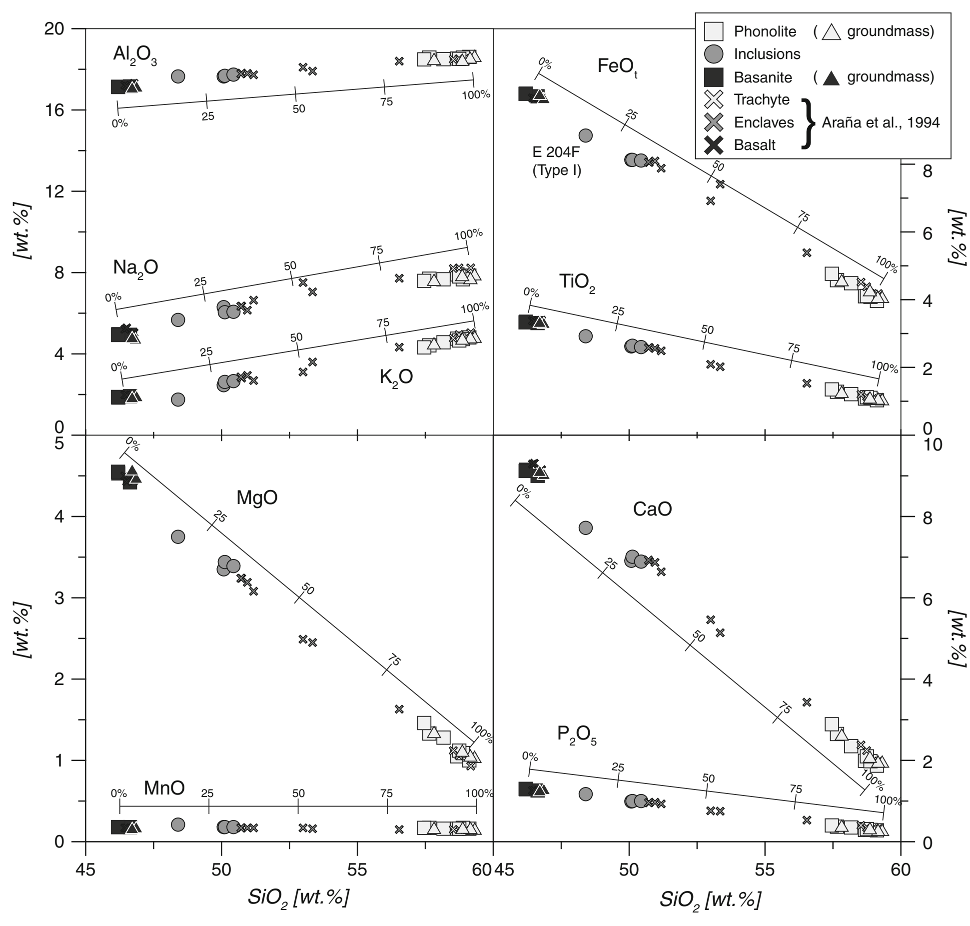

Fig. 4 Whole-rock major element composition of the Montaña Reventada eruption. Fe data recalculated to FeO_t using the formula $FeO_t = FeO + 0.899\ Fe_2O_3$ (Bence and Albee 1968). All major elements define straight trends when correlated to SiO_2, which indicates an origin of inclusions by mixing of the two principal components basanite and phonolite, rather than by fractional crystallisation. Note *graphical mixing lines* that indicate the percentage of phonolite material for intermediate compositions

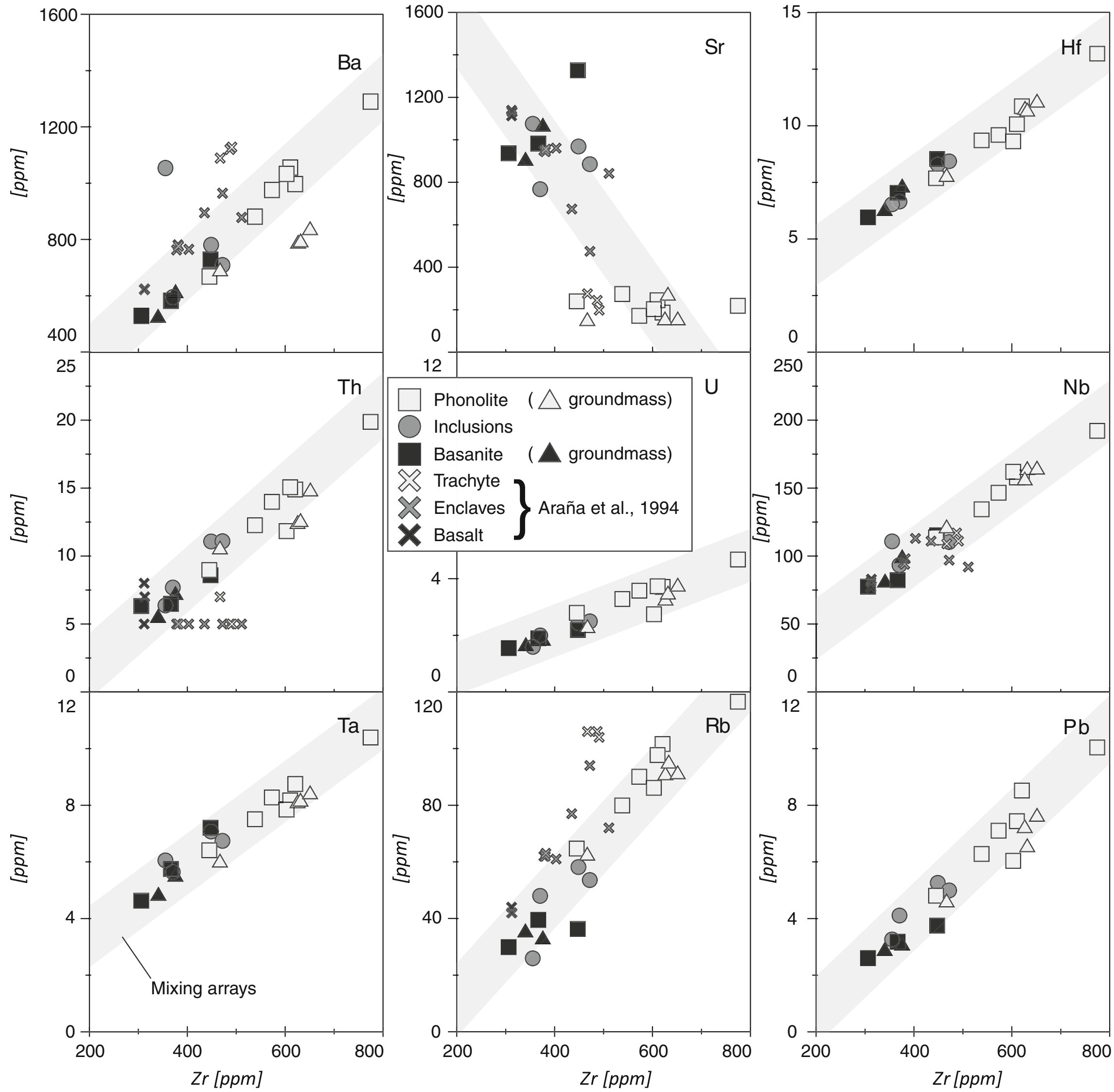

Fig. 5 Selected trace elements are plotted versus Zr concentration from Montaña Reventada. The *crosses* denote data from Araña et al. (1994) for comparison. Note the linear variation among the sample suite in most trace elements. Ba, Sr and Rb may be affected by crystal transfer of feldspar, the dominant mineral phase at Montaña Reventada. Phonolite samples are wide spread in trace elements, which is probably a result of diffusional hybridisation

samples overlap in their $^{207}Pb/^{204}Pb$ ratios (15.6122(34) to 15.6213(17) versus 15.6117(17) to 15.6196(29) versus 15.6168(30) to 15.6232(28), respectively). The $^{208}Pb/^{204}Pb$ ratios partially overlap between basanite, inclusions and phonolite (39.5423(43) to 39.5720(29) versus 39.5603(29) to 39.5858(46) versus 39.5769(39) to 39.5997(45), respectively), with each group reaching higher values. The results for Sr, Nd and Pb isotopes agree well with existing data for Tenerife igneous rocks (Palacz and Wolff 1989; Simonsen et al. 2000; Abratis et al. 2002; Gurenko et al. 2006). All errors are reported as 2SD (Table 1, online resource Table A1).

Discussion

Subaerial emplacement of lava

The basanite shows a chilled margin where the phonolite intruded (Fig. 1d), which indicates that the basanite was locally still hot at the time the phonolite was deposited. The gradational vesiculation of the phonolite for one metre upwards from the contact with the basanite indicates that either the heat coming from the freshly emplaced basanite caused inclusions and crystals within the phonolite to decompose (see inclusion degassing halos in Fig. 1g) or

Table 3 Percentages of two-component bulk mixtures between basanite and phonolite that reproduce inclusion compositions are given above

Inclusion	Basanite (%)	Phonolite (%)	Compared with calculated mixture	
			Enriched in	Depleted in
E206A	66	34	–	Li, Cu
E206B	66	34	–	Sc, Cu
E206D	66	34	–	–
E204F	80.4	19.6	Ba	Ni, Cu, Cs, Rb, U

Some trace elements were enriched or depleted in the real samples compared to the theoretical mixture, but variations remain unique to each sample

gas migrated upwards from the basanite into the phonolite. The basanite and the upper phonolite are thus effectively contemporaneous.

The lack of a basanite top breccia at the contact between the basanite and the phonolite indicates that this breccia is either not preserved or had never formed. The lack of a phonolite bottom breccia indicates, in turn, that it certainly never formed. Two scenarios are conceivable: (a) a rafting-type emplacement, where phonolite essentially floats on top of the ductile basanite. This would allow it to erode the basanite top breccia and explain the lack of a phonolite bottom breccia or (b) a continuous caterpillar-type emplacement, where the boundary between basanite and phonolite was never exposed to the surface, that is, both types of breccia never formed in the first place.

Flow-banded, angular inclusions (type IV) closely resemble the laminated texture of the underlying basanite. The phonolite may have picked up this clast type while overriding the basanite flow. Strictly speaking, type IV inclusions would then be a form of 'xenolith'. If this was the case, they would indicate a rafting-type emplacement of the phonolite lava.

Origin of intermediate magma

Major and trace element constraints

Whole-rock major element trends are linear for all oxide data from both datasets, Araña et al. (1994) and ours. Together they form an apparently continuous compositional sequence, bounded by the basanite and phonolite end-member compositions, with the inclusions plotting intermediate between them (Fig. 4). As the major element Harker patterns are exclusively straight, lacking the typical kinks expected from fractional crystallisation (cf. Geldmacher et al. 1998), hybridisation is thought to be the dominant process, i.e. physical and chemical mingling and mixing. De Campos et al. (2008) experimentally constrained the combined effects of incipient physical mingling and diffusion across an interface of two distinct magmas and found fluctuating geochemical trends (layering) between the end-member magmas at short time-scales of interaction (hours to days). By implication, a series of hybrid compositions that follows such straight trends as observed at Montaña Reventada can be regarded as being in an advanced stage of mixing, i.e. thoroughly hybridised. However, it needs to be taken into account that the data presented here are whole-rock samples, i.e. the effects of sample homogenisation have probably evened out intra-sample heterogeneities, thereby simplifying the observed geochemical relationships.

To check for interface processes, the phonolite *206Cont* was sampled just above the contact with the basanite. In some of the trace elements, the data from sample *206Cont* are indeed very low and overlap with some of the inclusions. In fact, the whole array of phonolite samples spreads out widely in some of their trace element concentrations, e.g. Zr, Ba, Rb, Pb, Nb and Ta (Fig. 5). In contrast, they cluster together in their major element concentrations (Fig. 4). The widely varying trace element concentrations in the phonolite indicate that diffusional interaction between the two magmas may still have occurred during cooling. The trace elements would have diffused either from abundant inclusions affecting the phonolite groundmass or across the contact between the main bodies of basanite and phonolite. In turn, the basanite appears comparatively free from such influence. One basanite sample contains significantly more Zr than the other basanites, but is consistent with the overall variation observed in recent Tenerife basanites, while the range of Zr observed in Reventada phonolite samples overlaps with and extends below the normal variation for Tenerife phonolites (Wiesmaier 2010).

Mass balance constraints

Trace element and major element oxide concentrations in inclusions were modelled as two-component bulk mixtures of basanite and phonolite. As basanite and phonolite samples are not completely compositionally uniform, we used their respective maximum and minimum concentrations for each

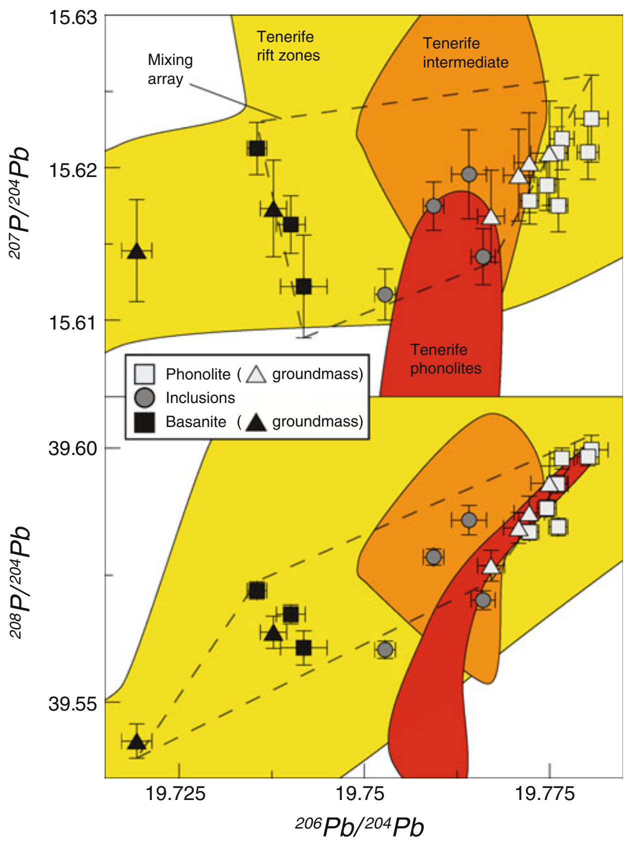

Fig. 6 Pb–Pb isotope systematics of the Montaña Reventada eruption. Errors are 2SD. Fields denote existing data from the Tenerife Teide-Pico Viejo complex and rift zones (Wiesmaier 2010): in yellow primitive rift zone basanites, in orange intermediate rocks and in red phonolites. Basanite and phonolite data from this study define independent subvertical trends. Mafic to intermediate inclusions that are found in the phonolites show a similar range in $^{207}Pb/^{204}Pb$ but bridge the gap in $^{206}Pb/^{204}Pb$ between the basanite and phonolite, consistent with a mixing origin. The basanite and phonolite end-members, in turn, define two parallel trends that do not overlap, characterising them as two genetically distinct magmas that define a mixing array

major and trace element. Mixtures of basanite and phonolite should fall within this interval of concentrations for both, major and trace elements.

In most major and trace elements, the inclusions from our dataset equate to mixtures of between 66:34 basanite to phonolite (E206A, E206B and E206D) and 80:20 basanite to phonolite (E204F). This is consistent with the graphical mixing solution in the Harker diagrams, where the three inclusions cluster together and the latter (E204F) shows a more mafic composition (Fig. 4). Two-component bulk mixing of basanite and phonolite yields matches for the major oxides SiO_2, MgO, Fe_2O_3 and TiO_2. The two less abundant major element oxides MnO and P_2O_5 are within 0.01 wt% of the model limits, which we deemed a satisfactory fit. The higher than expected concentration of Al_2O_3 and Na_2O in all inclusions is suggestive of added anorthoclase from the phonolite magma. Slightly lower K_2O concentrations than expected may be due to diffusion of K_2O towards the potassium-rich side of the diffusional interface (the phonolite), depleting the inclusion in this oxide (e.g. Watson and Baker 1991; Bindeman and Perchuk 1993; Araña et al. 1994; Bindeman and Davis 1999). Na and K concentrations that deviate from two-component bulk mixing patterns in inclusions and phonolite may thus also be affected by diffusion, which would be in line with the relatively enhanced diffusivities of these elements (Walker et al. 1981; Watson 1982; Walker and DeLong 1982; Lesher 1986; Lesher and Walker 1986).

The trace element concentrations in inclusions yield the same mixing ratios of 66:34 and 80:20 (mafic:felsic). Only a few elements deviate more than 10% from the linear two-component bulk mixing interval. Lithophile elements Li, Sc, Cs, Rb and U are depleted in inclusions. In addition to K_2O, Bindeman and Davis (1999) also constrained Li, Cs and Rb to diffuse from basalt to rhyolite melts (counter to the concentration gradient). The siderophile element Ni and the chalcophile element Cu are also depleted in the inclusions with respect to the mixing calculation (Table 3).

In the type I inclusion E204F, Ba is enriched relative to ideal mixing behaviour. As anorthoclase in Montaña Reventada phonolite contains large amounts of Ba (Table 2), this can be explained by the presence of anorthoclase crystals within this inclusion.

Sr and Nd isotopes

Although the inclusions occupy intermediate values between basanite and phonolite, all three rock types overlap in Sr and Nd isotopes by and large. The Montaña Reventada Sr and Nd isotope data nevertheless permit an origin of the mafic and intermediate inclusions by magma mixing (Online resource Table A1 and Fig. A3).

Pb isotopes

From our dataset ($n = 20$), all inclusion samples can be explained as mixtures between the basanite and phonolite end-members. The basanites, phonolites and inclusions show similar $^{207}Pb/^{204}Pb$ ratios, but systematic variation in $^{206}Pb/^{204}Pb$. This divides the components of Montaña Reventada into three arrays, with the mafic to intermediate inclusions placed in between the basanite and phonolite. On the balance of all geochemical and textural evidence, it is most probable that the inclusions have been produced through mixing of the two end-member compositions, basanite and phonolite (Fig. 6). A further implication of the significant difference in the observed Pb isotope ratios of basanite and phonolite is that they cannot be co-genetic. This is in line with constraints on the post-Icod-collapse sequence, of which Montaña Reventada forms part. The recent phonolite eruptions from the Teide-Pico Viejo central complex are thought to incorporate variable crustal components. Phonolite magmas in this recent Teide-Pico Viejo succession, while basanite from the Northeast and Northwest rift zones generally seems to remain largely unaffected by shallow level assimilation processes (Wiesmaier 2010).

Subsurface dynamics

Type I inclusions

Type I inclusions in Montaña Reventada phonolite are angular fragments of vesicle-rich, so-called mafic foam, indicating an interval of direct magmatic interaction prior to eruption. A large temperature contrast between hot, mafic and cooler, silicic magma may have induced fractions of mafic magma to quench rapidly upon contact between the two (cf. Bacon and Metz 1984; Bacon 1986). The resultant oversaturation of volatiles in the residual melt of quenched material can produce a foamy, vesiculate texture that shortly after may freeze completely (Eichelberger 1980). Exsolution of volatiles may then further enhance solidification in the residual melt (cf. Sparks 1997; Hammer et al. 2000). Geochemically, the type I inclusion E204F is anomalous relative to other inclusions in having a high Sr concentration and differences in other trace element concentrations. Sample E204F shows a multielement pattern that coincides with that of the basanite end-member. As diffusion is greatly hindered in solids compared to silicate liquids (Watson and Baxter 2007 and references therein), the basanite-like trace element pattern of inclusion E204F is consistent with a lesser degree of hybridisation, and this sample was most probably fully solidified soon after it was entrained in the phonolite magma. We thus interpret the type I inclusions as fragments of an initial, rapidly quenched contact between basanite and phonolite. By implication, the phonolite was probably rather cool at the time when the basanite first arrived. Subsequently, this almost solid, vesicular boundary zone was disrupted, creating the angular fragments of type I inclusions. This then would have permitted direct contact between the liquid portions of the basanite with the phonolite magma to give rise to the remaining types of inclusions. These show evidence of less severe temperature contrasts between a thermally more equilibrated basanite and phonolite pair.

Type II inclusions

Type II inclusions are indicative of a reduced, but still large temperature contrast. Instead of the angular outlines of the type I inclusions, the smooth and undulate contacts of type II inclusions preserve liquid textures. The pronounced temperature difference between the two bodies of magma, albeit not as strong as for type I inclusions, was still large enough to cause chilled margins to form (cf. Sparks et al. 1977; Eichelberger 1980; Marshall and Sparks 1984). The two magmas were therefore far from thermal equilibration, which implies a close temporal relationship between the formation of type I (mafic foam) and type II inclusions. We interpret type II inclusions as resulting from entrainment of mafic magma into “heated-up” and hence re-mobilised phonolite magma. Type II inclusions can only have formed after the mafic foam-bounding zone (i.e. the initial quenching) had been disrupted.

Type III inclusions

Type III inclusions may feature a lighter colour, along with filaments and blobs of darker, mafic magma within them (see Fig. 1f). Perugini et al. (2003) constrained the process of physical mixing (mingling) of two liquids of similar viscosity to be due to stretching and folding processes caused by internal movement of the liquids. The resulting textures in magmatic rocks consist of the so-called active regions, where intense mingling took place (filament textures), and coherent regions that remained largely unaffected by mingling (blob textures). The filaments and blobs in type III inclusions are thus most probably the result of physical mingling of basanite and phonolite. As suggested by Perugini et al. (2003), this may have been facilitated by a cooled basanite and a heated-up phonolite, i.e. converging viscosities and temperatures that allowed mingling of compositionally distinct batches of magma. Sieve textures in anorthoclases within the phonolite are indicative of such an increase in temperature (cf. Hibbard 1995; Stewart and Pearce 2004). These anorthoclase crystals are also observed within the inclusions (Table 2, online resource Fig. A1) as direct evidence for a disequilibrium mineral assemblage, i.e. liquid–liquid interaction between basanite and phonolite including crystal transfer (e.g. Gamble 1979; Tepley et al. 1999; Troll and Schmincke 2002; Troll et al. 2004; Browne et al. 2006; Meade et al. 2009). This is in line with several studies that have suggested that thorough mixing of two compositionally distinct magmas requires physical mingling before diffusion may even out the remaining chemical and textural heterogeneities (e.g. Kouchi and Sunagawa 1985; Perugini et al. 2003; Zimanowski et al. 2004). In their numerical model, Perugini et al. (2003) correlated the resulting features of intense mingling (active and coherent regions) to natural examples of magma mingling at the islands of Salina, Vulcano and Lesbos. The comprehensive micro-analytical study conducted by Perugini et al. (2003) of these natural equivalents of their experiments show that active regions (filaments) may be equilibrated easily by the resultant diffusion due to their large interfacial parameter and highly fractal nature, while the coherent regions (inclusions) remain largely unaffected by diffusion. To achieve a good degree of mixing of two magmas within a short timeframe, it therefore appears to be paramount that intense physical mingling takes place initially during efficient hybridisation. We interpret type III inclusions as the result of physical interaction between the basanite and the phonolite magma, showing that not only was diffusive hybridisation at work as suggested by Araña et al. (1994), but also physical magma mixing.

Nevertheless, diffusional processes must have played a role in the hybridisation of the inclusions. The magnitude of the compositional gradient that persists between a basanite and a phonolite magma has been shown to trigger considerable amounts of diffusive equilibration (Koyaguchi 1989). This was likely the case for type III blob-like inclusions, featuring diffuse margins. Furthermore, the high surface-volume ratio of the inclusions enhances their potential for diffusional equilibration. Most likely, an interplay of both diffusion and magma mixing gave rise to the observed intermediate compositions in the inclusions. However, the much shorter timeframe necessary for hybridisation when mingling is part of the mixing process has implications for the configuration of the magma chamber prior to mixing.

Timescale of inclusion formation

The transition from formation of mafic foam over quenching to chilled margins to final liquid–liquid interaction observed in the inclusions indicates a rapid succession of events. The formation of chilled margins in type II inclusions swiftly succeeded the initial formation of quench-type inclusions, for the thermal contrast was still strong enough to allow forming chilled margins. The transition between type II and type III inclusions is less clear, but a close temporal relationship seems likely, too. By using the MELTS algorithm in combination with cooling and decompression experiments, Coombs et al. (2003) temporally constrained the formation of inclusions and chilled margins between an andesite and a dacite to be on the order of hours only. Prolonged contact would thereafter lead to solidification of the undercooled andesite. By analogy, the duration of mixing at Montaña Reventada was probably on a similar order of magnitude (hours to days). A long-lived, stratified magma chamber, which possessed a stable, diffusive interface between the two main magmas and thermally equilibrated and crystallised for months to years prior to eruption, is inconsistent with a timescale of interaction between basanite and phonolite that lasted from a few hours to perhaps days at Montaña Reventada.

Magma chamber configuration

The amount of mixing that took place appears to be rather restricted as inclusions are estimated to amount to less than 1 vol% of the total deposit volume (Araña et al. 1994). Furthermore, the groundmasses of basanite and phonolite lack the typical mingling features, like the folded over filaments of distinct types of magma adjacent to each other (cf. Perugini et al. 2003). The occurrence of light-coloured phonolitic material within the basanite is rare and restricted to sheared inclusions, which probably originated from phonolite intruding the underlying basanite during subaerial flow. This means that, in contrast to the hybrid inclusions, the massive basanite and phonolite lavas are comparatively free of physical mixing.

Campbell and Turner (1986) experimentally constrained the effects of viscosity on magma mixing and concluded that two magmas being mixed need to possess comparable viscosities in order to efficiently mix large volumes of them. At Montaña Reventada, the magmas initially possessed very different viscosities, however. The basanite is vesicle rich in places and the mafic inclusions within the phonolite often show degassing halos, indicating an elevated volatile content and potentially reduced basanite viscosity prior to gas release. As a result, the viscosity difference between basanite and phonolite may have been much more pronounced. In the case of differing viscosities in the two end-member magmas, Campbell and Turner (1986) suggested that superheating of the felsic end-member (and concurrent cooling of the mafic magma) allows for approaching viscosities and facilitates mingling. According to these authors, this may occur either in long-lived, stratified magma chambers or as a spatially restricted phenomenon during fountaining or forced intrusion, creating a small-volume, hybrid boundary layer between mafic and felsic magma. In the case of Montaña Reventada, a rather short period of interaction is indicated, consistent with the relatively small volume of hybrid inclusions that occurs within the host phonolite. Mingling of basanite and phonolite appears to have been restricted to a spatially small zone of interaction, and after an initial carapace of quenched basanite (mafic foam) had been disaggregated. Hence, instead of a long-lived, stratified magma chamber, a forced intrusion (fountaining?) of basanite into the ambient phonolite liquid appears the more likely option at Montaña Reventada.

Mixing mechanism

In a comparable case to Montaña Reventada (mafic erupts before felsic), Pinatubo erupted andesite before dacite in

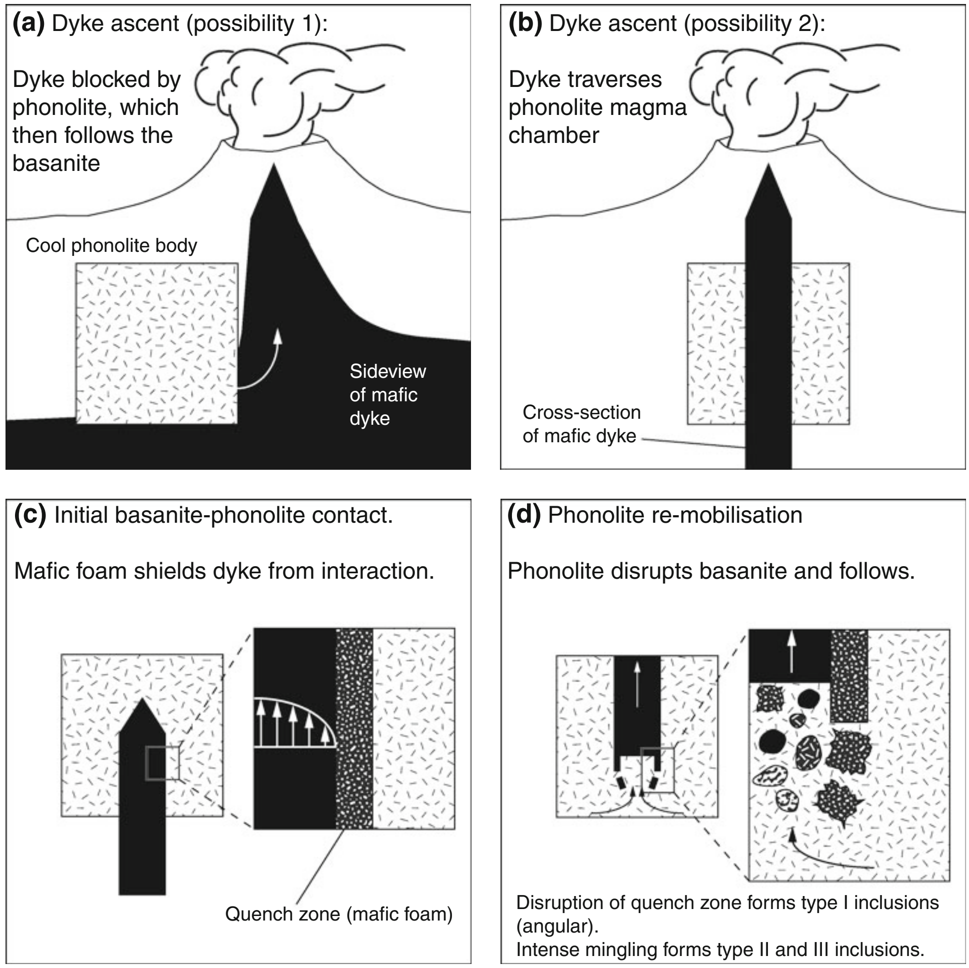

Fig. 7 Sketch of subsurface dyke ascent and magma chamber dynamics. At Montaña Reventada, two possibilities of dyke ascent are conceivable: **a** A basanite dyke is blocked by a phonolite body, but continues to ascend in the periphery of the previously emplaced phonolite or **b** a basanite dyke cuts through a cool phonolite magma chamber. **c** and **d** are schematic representations of the immediate contact between basanite and phonolite and apply for both modes of dyke ascent. **c** At first contact between basanite and phonolite, the basanite develops a vesicular, solid layer of quenched material (mafic foam) that isolates the bulk of the basanite from interaction with the phonolite. The lifespan of this screen of quenched material may be short though. **d** Both magmas equilibrate thermally, thus remobilising the phonolite. After the basanite eruption wanes, the phonolite exploits the pre-established conduit, collecting angular fragments of mafic foam and mingling with the remains of liquid basanite on the way to the surface

1991, the latter of which comprises the bulk of the final deposit (Pallister et al. 1992). Snyder and Tait (1996) tested the Pinatubo scenario experimentally by using a mechanism invoked by Huppert et al. (1983, 1984); the viscous coupling of magmas driven by thermal convection. Snyder and Tait (1996) applied this mechanism to the transient phase of replenishment of a magma chamber and found that a strong temperature contrast between replenishing mafic and ambient felsic magma may trigger local convection within the felsic member, thereby entraining mafic liquid by viscous coupling. Their analogue liquid of mafic magma reached the roof of the chamber as a mixed layer, like so providing a model for the eruption of mixed andesite erupting before pristine dacite, as at Pinatubo in 1991.

However, at Montaña Reventada, the temperature contrast between basanite and phonolite may have been larger compared to the one between andesite and dacite at Pinatubo, as indicated by the ubiquitous type I and type II inclusions. Only few chilled margin inclusions have been found at Pinatubo, hence, quenching appears to have been more dominant at Reventada. Furthermore, the first-erupting andesite at Pinatubo is of hybrid origin, while, intriguingly, the Reventada basanite appears texturally and compositionally pristine. Apart from what was left within the plumbing system, the basanite at Reventada had erupted in its entirety *before* the phonolite (no more basanite followed after phonolite). In fact, the last basanite material to erupt had been carried to the surface by the phonolite, being the inclusions that we interpret to originate from initial contact between the two magmas. In other words, the phonolite collected the leftover basanite material that had initially quenched and continued to interact. This means, the basanite either largely bypassed the phonolite chamber at its side, only tapping it peripherally (Fig. 7a), or it traversed the phonolite body without any major form of interaction, after which the phonolite followed the basanite through its conduit (Fig. 7b).

Could it thus be that the initial quenching formed a carapace around the basanite dyke (perhaps comparable to the formation of pillow lavas underwater), permitting it to traverse through the body of stiff phonolite? At Montaña Reventada, the phonolite was probably rather cool before interaction, indicating a high viscosity body into which a basanite intruded. The basanite would quench at the interface to the phonolite (mafic foam, type I inclusions, Fig. 7c). Type II inclusions would form when the re-mobilised phonolite would have entered the established basanite conduit, collecting the fragments of the former quench zone (type I inclusions) and interacting with the liquid basanite magma that is left within the conduit. Because of the ongoing thermal interaction between the phonolite and the basanite, the temperature contrast progressively lowered. This ongoing thermal equilibration allowed for approaching viscosities and progressively permitted mingling to form type III inclusions (Fig. 7d). For example, the default type of eruption in the Katmai region, Alaska, has been described as small, andesite magma chambers, into which mafic replenishment occur. At low recharge vigour, the basalt mixes with the andesite. However, when unmixed mafic scoria is erupted, this is interpreted as basalt magma passing through the andesite chamber without major interaction (Coombs et al. 2000; Eichelberger and Izbekov 2000). The crucial question for this model to work is whether such a carapace of mafic foam may persist for a short time or if it would be disrupted instantly.

Equally plausible appears the notion that the basanite was blocked by the phonolite chamber, thereby partly intruding it, but eventually continuing to ascend to the side of it. Again, type I inclusions would have formed at initial contact, while type II and type III would have been generated when the re-heated phonolite exploited the basanite conduit afterwards. Examples for a similar scenario have been found at Karymsky (Kamchatka), Katmai/Novarupta centre (Alaska) and also the recent Eyjafjallajökull/Fimmvörðuháls eruption in Iceland, where mafic dykes first opened a fissure at the flank of these volcanoes before triggering more silicic eruptions from central vents Eichelberger and Izbekov 2000; Gertisser 2010; Sigmundsson et al. 2010).

Model

We envisage a pre-existing phonolite magma pocket, belonging to the central Teide-Pico Viejo complex that was cut by an ascending mafic dyke of the NW rift zone (Fig. 7a, b). The phonolite had formed by processes that are unrelated to the basanite and the two magmas met just prior to eruption. The distinct Pb isotope signatures of basanite and phonolite magmas support the view that both magmas were co-eruptive, but not co-genetic. When the basanite dyke intruded the phonolite magma chamber, it partly quenched against it, leaving behind solidified, vesicular mafic inclusions within the phonolite and liquid basanite magma that was entrained into the phonolite liquid. This gave rise to type II and type III mafic inclusions that were hybridised by mingling and mineral exchange along with diffusion. Apart from the resulting hybrid inclusions, both end-members remained mechanically and chemically distinct.

The Montaña Reventada composite flow is a direct manifestation of the petrogenetic bimodality in recent Tenerife activity. Reventada is located above the assumed boundary of the central Teide-Pico Viejo complex with the NW rift zone. In recent times, Teide and Pico Viejo erupted phonolite from shallow magma chambers ($\sim$sea level, e.g. Ablay et al. 1998), whereas the rift zones continued to produce lavas of primitive composition that ascended in dykes from upper mantle or lower crustal levels (Carracedo et al. 2007). In the border zone between these two plumbing systems, not only Montaña Reventada shows a lower mafic and an upper felsic member, but the lavas of Cuevas Negras do so as well and also erupted successively during a single event (Carracedo et al. 2008).

Conclusions

Our study of the Montaña Reventada composite lava flow shows that intermediate magmas in Tenerife may form through direct interaction of two end-member-type magmas: basanite and phonolite. At Montaña Reventada, hybridisation remained volumetrically incomplete as mixing was interrupted by eruption, and inclusions reflect short-term interaction between basanite and phonolite. Prolonged interaction of basanite and phonolite would likely lead to homogenisation of the liquid magma portions and may be one of the processes responsible to produce intermediate magmas in ocean islands such as the Canary archipelago. Montaña Reventada represents a case, where a mafic dyke encountered a previously emplaced phonolite pocket. The basanite must have either traversed or bypassed the phonolite chamber after initial contact, with basanite erupting first, followed by phonolite. The eruption occurred in the transition zone between the central, phonolite-erupting Teide-Pico Viejo complex and the basanite-erupting NW rift zone, implying that two genetically distinct magmas have accidentally met to form this composite eruption. This raises the possibility of small-volume phonolite magma chambers being emplaced at shallow levels within the current magmatic plumbing system in Tenerife.

Acknowledgments Carmela Freda and Alejandro Rodríguez-González helped with the interpretation of field evidence. Audray Delcamp is thanked for help in sample preparation. We are grateful to G. Davies, L. Font and R. Smeets for technical support in Amsterdam and B. van der Wagt for ICP-MS and MC-ICP-MS analyses, also in Amsterdam. Chris Harris revised an early version of this manuscript. We thank Cristina De Campos and two anonymous reviewers for their thoughtful comments. This project forms part of the PhD theses of SW and FMD and was supported by a scholarship from the School of Natural Sciences at Trinity College Dublin to SW and a Science Foundation Ireland grant to VRT. We also acknowledge further support from the Boldy/Johnston award from the Department of Geology, Trinity College Dublin to SW and the Plan Nacional I + D+I, project CGL 2008-02842/BTE, and Caja Canarias, Tenerife, Spain to JCC.

References

Ablay GJ, Carroll MR, Palmer MR, Martí J, Sparks RSJ (1998) Basanite-Phonolite Lineages of the Teide-Pico Viejo Volcanic Complex, Tenerife, Canary Islands. J Petrol 39(5):905–936

Abratis M, Schmincke HU, Hansteen T (2002) Composition and evolution of submarine volcanic rocks from the central and western Canary Islands. Int J Earth Sci 91(4):562–582

Araña V, Aparicio A, Garcia Cacho L, Garcia Garcia R (1989) Mezcla de magmas en la región central de Tenerife. In: Araña V, Coello J (eds) Los volcanes y la caldera del Parque Nacional del Teide (Tenerife, Islas Canarias), Vol. Ministerio de Agricultura Pesca y Alimentación, pp 269–298

Araña V, Martí J, Aparicio A, García-Cacho L, García-García R (1994) Magma mixing in alkaline magmas: an example from Tenerife, Canary Islands. Lithos 32(1–2):1–19

Bacon CR (1986) Magmatic inclusions in silicic and intermediate volcanic rocks. J Geophys Res 91(B6):6091–6112

Bacon CR, Metz JM (1984) Magmatic inclusions in rhyolites, contaminated basalts, and compositional zonation beneath the Coso volcanic field, California. Contrib Miner Petrol 85:346–365

Baker DR (1990) Chemical interdiffusion of dacite and rhyolite: anhydrous measurements at 1 atm and 10 kbar, application of transition state theory, and diffusion in zoned magma chambers. Contrib Miner Petrol 104(4):407–423

Bas MJL, Maitre RWL, Streckeisen A, Zanettin B, ISotSoI Rocks (1986) A chemical classification of volcanic rocks based on the total alkali-silica diagram. J Petrol 27(3):745–750

Bence AE, Albee AL (1968) Empirical correction factors for the electron microanalysis of silicates and oxides. J Geol 76(4): 382–403

Bindeman IN, Davis AM (1999) Convection and redistribution of alkalis and trace elements during the mingling of basaltic and rhyolitic melts. Petrol 7(1):91–101

Bindeman IN, Perchuk LL (1993) Experimental studies of magma mixing at high pressures. Int Geol Rev 35:721–733

Blake S (1981a) Eruptions from zoned magma chambers. J Geol Soc (London, UK) 138(3):281–287

Blake S, Ivey GN (1986) Magma-mixing and the dynamics of withdrawal from stratified reservoirs. J Volcanol Geotherm Res 27(1–2):153–178

Brian S, Geoffrey T, Margaret S, John NL (1980) Analysis of geologic materials using an automated x-ray fluorescence system. X-Ray Spectr 9(4):198–205

Browne BL, Eichelberger JC, Patino LC, Vogel TA, Uto K, Hoshizumi H (2006) Magma mingling as indicated by texture and Sr/Ba ratios of plagioclase phenocrysts from Unzen volcano, SW Japan. J Volcanol Geotherm Res 154(1–2):103–116

Calanchi N, Rosa R, Mazzuoli R, Rossi P, Santacroce R, Ventura G (1993) Silicic magma entering a basaltic magma chamber: eruptive dynamics and magma mixing—an example from Salina (Aeolian islands, Southern Tyrrhenian Sea). Bull Volcanol 55(7):504–522

Campbell IH, Turner JS (1986) The Influence of viscosity on fountains in Magma chambers. J Petrol 27(1):1–30

Carracedo JC (1994) The Canary Islands: an example of structural control on the growth of large oceanic-island volcanoes. J Volcanol Geotherm Res 60(3–4):225

Carracedo JC, Rodríguez Badiola E, Guillou H, Paterne M, Scaillet S, Pérez Torrado FJ, Paris R, Fra-Paleo U, Hansen A (2007) Eruptive and structural history of Teide Volcano and Rift zones of Tenerife, Canary Islands. Geol Soc Am Bull 119(9):1027–1051

Carracedo JC, Rodríguez Badiola E, Guillou H, Paterne M, Scaillet S, Pérez Torrado FJ, Paris R, Rodríguez González A, Socorro S (2008) El Volcán Teide—Volcanología, Interpretación de Pasajes y Iterinarios Comentados, vol. Caja Generál de Ahorros de Canarias

Coombs ML, Eichelberger JC, Rutherford MJ (2000) Magma storage and mixing conditions for the 1953–1974 eruptions of Southwest Trident volcano, Katmai National Park, Alaska. Contrib Miner Petrol 140(1):99–118

Coombs ML, Eichelberger JC, Rutherford MJ (2003) Experimental and textural constraints on mafic enclave formation in volcanic rocks. J Volcanol Geotherm Res 119(1–4):125–144

Crank J (1975) The mathematics of diffusion, vol. Clarendon, Oxford

De Campos CP, Dingwell DB, Perugini D, Civetta L, Fehr TK (2008) Heterogeneities in magma chambers: Insights from the behaviour of major and minor elements during mixing experiments with natural alkaline melts. Chem Geol 256(3–4):131–145

Eggins SM, Woodhead JD, Kinsley LPJ, Mortimer GE, Sylvester P, McCulloch MT, Hergt JM, Handler MR (1997) A simple method for the precise determination of $>=40$ trace elements in geological samples by ICPMS using enriched isotope internal standardisation. Chem Geol 134(4):311–326

Eichelberger JC (1980) Vesiculation of mafic magma during replenishment of silicic magma reservoirs. Nature 288(5790):446–450

Eichelberger JC, Izbekov PE (2000) Eruption of Andesite triggered by Dyke injection: contrasting cases at Karymsky Volcano, Kamchatka and Mt Katmai, Alaska. Philos Trans R Soc London, Ser A 358(1770):1465–1485

Eichelberger JC, Chertkoff DG, Dreher ST, Nye CJ (2000) Magmas in collision: rethinking chemical zonation in silicic magmas. Geology 28(7):603–606

Elburg M, Vroon P, van der Wagt B, Tchalikian A (2005) Sr and Pb isotopic composition of five USGS glasses (BHVO-2G, BIR-1G, BCR-2G, TB-1G, NKT-1G). Chem Geol 223(4):196–207

Freundt A, Schmincke H-U (1992) Mixing of rhyolite, trachyte and basalt magma erupted from a vertically and laterally zoned reservoir, composite flow P1, Gran Canaria. Contrib Miner Petrol 112(1):1–19

Gamble JA (1979) Some relationships between coexisting granitic and basaltic magmas and the genesis of hybrid rocks in the Tertiary central complex of Slieve Gullion, Northeast Ireland. J Volcanol Geotherm Res 5(3–4):297–316

Geldmacher J, Haase KM, Devey CW, Garbe-Schönberg CD (1998) The petrogenesis of Tertiary cone-sheets in Ardnamurchan, NW Scotland: petrological and geochemical constraints on crustal contamination and partial melting. Contrib Miner Petrol 131(2):196–209

Gertisser R (2010) Eyjafjallajökull volcano causes widespread disruption to European air traffic. Geol Today 26(3):94–95

Gurenko AA, Hoernle KA, Hauff F, Schmincke HU, Han D, Miura YN, Kaneoka I (2006) Major, trace element and Nd-Sr-Pb-O-He-Ar isotope signatures of shield stage lavas from the central and western Canary Islands: Insights into mantle and crustal processes. Chem Geol 233(1–2):75–112

Hammer JE, Cashman KV, Voight B (2000) Magmatic processes revealed by textural and compositional trends in Merapi dome lavas. J Volcanol Geotherm Res 100(1–4):165–192

Harvey PK, Taylor DM, Hendry RD, Bancroft F (1973) An accurate fusion method for the analysis of rocks and chemically related materials by X-ray fluorescence spectrometry. X-Ray Spectrom 2(1):33–44

Hibbard MJ (1995) Petrography to Petrogenesis, vol. Prentice Hall, Englewood Cliffs, p 587

Hildreth EW (1979) The Bishop Tuff: evidence for the origin of compositional zonation in silicic magma chambers. Geol Soc Spec Publ 180:43–75

Hildreth W (1981) Gradients in Silicic Magma chambers: implications for Lithospheric magmatism. J Geophys Res 86(B11): 10153–10192

Huppert HE, Turner JS, Stephen R, Sparks J (1982) Replenished magma chambers: effects of compositional zonation and input rates. Earth Planet Sci Lett 57(2):345–357

Huppert HE, Sparks RSJ, Turner JS (1983) Laboratory investigations of viscous effects in replenished magma chambers. Earth Planet Sci Lett 65(2):377–381

Huppert HE, Stephen R, Sparks J, Turner JS (1984) Some effects of viscosity on the dynamics of replenished magma chambers. J Geophys Res 89(B8):6857–6877

Izbekov PE, Eichelberger JC, Ivanov BV (2004) The 1996 Eruption of Karymsky Volcano, Kamchatka: historical record of Basaltic replenishment of an Andesite Reservoir. J Petrol 45(11): 2325–2345

Kouchi A, Sunagawa I (1985) A model for mixing basaltic and dacitic magmas as deduced from experimental data. Contrib Miner Petrol 89(1):17–23

Koyaguchi T (1989) Chemical gradient at diffusive interfaces in magma chambers. Contrib Miner Petrol 103(2):143–152

Kuritani T (2001) Replenishment of a mafic magma in a zoned felsic magma chamber beneath Rishiri Volcano, Japan. Bull Volcanol 62(8):533–548

Lesher CE (1986) Effects of silicate liquid composition in mineral-liquid element partitioning from Soret diffusion studies. J Geophys Res 91:6123–6141

Lesher CE, Walker D (1986) Solution properties of silicate liquids from thermal diffusion experiments. Geochim Cosmochim Acta 50:1397–1411

Luais B, Telouk P, Albaréde F (1997) Precise and accurate neodymium isotopic measurements by plasma-source mass spectrometry. Geochim Cosmochim Acta 61(22):4847–4854

Marshall LA, Sparks RSJ (1984) Origin of some mixed-magma and net-veined ring intrusions. J Geol Soc (London, UK) 141(1): 171–182

McDonough WF, Ss Sun (1995) The composition of the earth. Chem Geol 120(3–4):223–253

Meade FC, Chew DM, Troll VR, Ellam RM, Page LM (2009) Magma Ascent along a major terrane boundary: crustal contamination and Magma mixing at the Drumadoon Intrusive complex, Isle of Arran, Scotland. J Petrol 50(12):2345–2374

Norrish K, Hutton JT (1969) An accurate X-ray spectrographic method for the analysis of a wide range of geological samples. Geochim Cosmochim Acta 33(4):431–453

Palacz ZA, Wolff JA (1989) Strontium, neodymium and lead isotope characteristics of the Granadilla Pumice, Tenerife: a study of the causes of strontium isotope disequilibrium in felsic pyroclastic deposits. Geol Soc Spec Publ 42(1):147–159

Pallister JS, Hoblitt RP, Reyes AG (1992) A basalt trigger for the 1991 eruptions of Pinatubo volcano? Nature 356(6368):426–428

Perugini D, Poli G, Mazzuoli R (2003) Chaotic advection, fractals and diffusion during mixing of magmas: evidence from lava flows. J Volcanol Geotherm Res 124(3–4):255–279

Pin C, Briot D, Bassin C, Poitrasson F (1994) Concomitant separation of strontium and samarium-neodymium for isotopic analysis in silicate samples, based on specific extraction chromatography. Anal Chim Acta 298(2):209–217

Raczek I, Jochum KP, Hofmann AW (2003) Neodymium and strontium isotope data for USGS reference materials BCR-1, BCR-2, BHVO-1, BHVO-2, AGV-1, AGV-2, GSP-1, GSP-2 and eight MPI-DING reference glasses. Geostandards Newslett 27:173–179

Sigmundsson F, Hreinsdottir S, Hooper A, Arnadottir T, Pedersen R, Roberts MJ, Oskarsson N, Auriac A, Decriem J, Einarsson P, Geirsson H, Hensch M, Ofeigsson BG, Sturkell E, Sveinbjornsson H, Feigl KL (2010) Intrusion triggering of the 2010 Eyjafjallajökull explosive eruption. Nature 468:426–430

Simonsen SL, Neumann ER, Seim K (2000) Sr-Nd-Pb isotope and trace-element geochemistry evidence for a young HIMU source and assimilation at Tenerife (Canary Island). J Volcanol Geotherm Res 103(1–4):299–312

Smith RL (1979) Ash-flow magmatism. Geol Soc Spec Publ 180:5–27

Smith R, Bailey R (1966) The Bandelier Tuff: a study of ash-flow eruption cycles from zoned Magma chambers. Bull Volcanol 29(1):83–103

Snyder D, Tait S (1996) Magma mixing by convective entrainment. Nature 379(6565):529–531

Sparks RSJ (1997) Causes and consequences of pressurisation in lava dome eruptions. Earth Planet Sci Lett 150:177–189

Sparks SRJ, Sigurdsson H, Wilson L (1977) Magma mixing: a mechanism for triggering acid explosive eruptions. Nature 267(5609):315–318

Stewart ML, Pearce TH (2004) Sieve-textured plagioclase in dacitic magma: Interference imaging results. Am Miner 89:348–351

Tepley FJ III, Davidson JP, Clynne MA (1999) Magmatic interactions as recorded in Plagioclase Phenocrysts of Chaos Crags, Lassen Volcanic Center, California. J Petrol 40(5):787–806

Troll VR, Schmincke HU (2002) Magma mixing and crustal recycling recorded in Ternary Feldspar from compositionally Zoned Peralkaline Ignimbrite 'A', Gran Canaria, Canary Islands. J Petrol 43(2):243–270

Troll VR, Donaldson CH, Emeleus CH (2004) Pre-eruptive magma mixing in ash-flow deposits of the Tertiary Rum Igneous Centre, Scotland. Contrib Miner Petrol 147(6):722–739

Turner JS (1980) A fluid-dynamical model of differentiation and layering in magma chambers. Nature 285(5762):213–215

Turner JS, Campbell IH (1986) Convection and mixing in magma chambers. Earth Sci Rev 23(4):255–352

Turner SP, Platt JP, George RMM, Kelley SP, Pearson DG, Nowell GM (1999) Magmatism associated with Orogenic Collapse of the Betic-Alboran Domain, SE Spain. J Petrol 40(6):1011–1036

Walker D, DeLong SE (1982) Soret separation of mid-ocean ridge basalt magma. Contrib Miner Petrol 79:231–240

Walker D, Lesher CE, Hays JF (1981) Soret separation of lunar liquids. In: Lunar and planetary science XII, vol, pp 991–999

Watson EB (1982) Basalt contamination by continental crust: some experiments and models. Contrib Miner Petrol 80:73–87

Watson EB, Baker DR (1991) Chemical diffusion in Magmas: an overview of experimental results and geochemical applications. In: Perchuk LL, Kushiro I (eds) Advances in physical geochemistry, vol 6. Springer, New York, pp 120–151

Watson EB, Baxter EF (2007) Diffusion in solid-earth systems. Earth Planet Sci Lett 253(3–4):307–327

Weis D, Kieffer B, Maerschalk C, Barling J, de Jong J, Williams GA, Hanano D, Pretorius W, Mattielli N, Scoates JS, Goolaerts A, Friedman RM, Mahoney JB (2006) High-precision isotopic characterization of USGS reference materials by TIMS and MC-ICP-MS. Geochem Geophys Geosyst 7(8):Q08006

Wiesmaier S (2010) Magmatic differentiation and bimodality in oceanic island settings—implications for the petrogenesis of

magma in Tenerife, Spain. PhD Thesis, Dept. Of Geology, Trinity College Dublin, p 191
Wolff JA, Storey M (1984) Zoning in highly alkaline magma bodies. Geol Mag 121(6):563–575
Wolff JA, Grandy JS, Larson PB (2000) Interaction of mantle-derived magma with island crust? Trace element and oxygen isotope data from the Diego Hernandez Formation, Las Canadas, Tenerife. J Volcanol Geotherm Res 103(1–4):343–366
Zimanowski B, Büttner R, Koopmann A (2004) Experiments on magma mixing. Geophys Res Lett 31(9):L09612